Chemosphere 367 (2024) 143665

Contents lists available at ScienceDirect

Chemosphere

journal homepage: www.elsevier.com/locate/chemosphere

Evaluation of the impact of L-Tryptophan on the toxicology of Perfluorooctanoic acid in Daphnia magna: Characterization and perspectives

Mathieu Verhille [a,b,*], Robert Hausler [a,b]

[a] Department of Civil and Environmnetal Engineering, École de Technologie Supérieure University of Québec, Montréal, Québec, H3C 1K3, Canada
[b] Station Expérimentale des Procédés Pilotes en Environnement (STEPPE-ÉTS, École de Technologie Supérieure), Montréal, Québec, H3C 1K3, Canada

HIGHLIGHTS

- Dissolved L-Trp significantly reduces acute PFOA toxicity in *Daphnia magna.*
- Optimal L-Trp molar ratio (0.5–1) effectively reduces toxicological effects of PFOA.
- L-Trp and PFOA form a weakly bound complex, mitigating PFOA toxicity.
- Van der Waals forces and hydrogen bonds dominate in the L-Trp/PFOA complex.

GRAPHICAL ABSTRACT

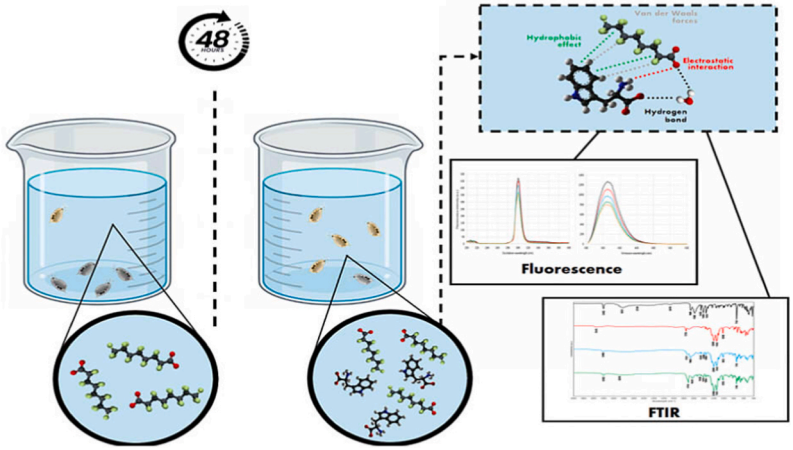

ARTICLE INFO

Keywords:
Perfluorooctanoic acid
Tryptophan
Daphnia magna
Toxicity effect
Non-covalent interactions

ABSTRACT

Perfluorooctanoic acid (PFOA) is a pervasive environmental contaminant with well-documented toxic effects on both humans and animals, attracting significant scientific concern. Due to its affinity for proteins, research has predominantly focused on PFOA's interactions with biological macromolecules. However, the specific role of smaller molecules, such as amino acids, remains underexplored. This study uniquely evaluates the potential of L-tryptophan (L-Trp) to mitigate PFOA toxicity and investigates the interaction mechanisms involved. Results indicate that the presence of L-Trp in PFOA-contaminated water reduces acute toxicity in *Daphnia magna*, with an optimal molar ratio of approximately 1:2 (Trp:PFOA). The findings reveal that non-covalent interactions, particularly van der Waals forces and hydrogen bonds, are central to the Trp–PFOA complex formation. Additional contributions from hydrophobic interactions at the indole group and electrostatic forces between carbonyl and amine groups further stabilize the complex. These interactions likely reduce PFOA's toxicity by altering its bioavailability and distribution. While this study offers valuable insights into the binding mechanisms between L-

* Corresponding author. 1100 R. Notre Dame O, Montréal, QC H3C 1K3, Canada.
E-mail address: mathieu.verhille1@ens.etsmtl.ca (M. Verhille).

https://doi.org/10.1016/j.chemosphere.2024.143665
Received 23 August 2024; Received in revised form 13 October 2024; Accepted 31 October 2024
Available online 6 November 2024

Trp and PFOA, it raises important questions about the reversibility of this interaction and its applicability to other per- and polyfluoroalkyl substances (PFASs).

1. Introduction

PFOA, with formula $C_8HF_{15}O_2$, is a synthetic molecule belonging to the perfluorinated carboxylic acid (PFCA) family, characterized by a perfluoroalkyl chain and a carboxylate end group. Renowned for its chemical and thermal resistance properties, as well as its amphipathic nature, PFOA has been widely used in a variety of industrial and domestic applications (Sunderland et al., 2019). Its high C–F bond stability, coupled with nearly six decades of use, has made it one of the most widely detected PFASs in the global environment and in humans (Manojkumar et al., 2023; Pan et al., 2018). This wide distribution, coupled with its environmental persistence (Kwak et al., 2020), raises significant concerns about its toxic effects, highlighting the urgent need to understand and mitigate the ecological impacts of this compound (Ankley et al., 2021).

The toxicological effects (hepatotoxicity, immunotoxicity, malformations, etc.) of PFASs are now well-established (Kang et al., 2019; Lau, 2015; Pérez et al., 2013; Steenland et al., 2020). However, the mechanisms involved are still insufficiently documented (Ankley et al., 2021). Their increasing concentrations along food webs (Li et al., 2023), correlated with their amphiphilic character, has suggested their ability to bioaccumulate. In particular, PFASs bioaccumulation has been shown to increase with perfluoroalkyl chain length (Bertin et al., 2014; Du et al., 2021). Accordingly, some studies have focused on their proteinophilic properties (Death et al., 2021; Wen et al., 2016; Zhao et al., 2023). In situ and in vivo studies have shown that some PFASs, such as PFOA, exhibit a high affinity for serum albumin, as well as fatty acid-related proteins, and accumulate in protein-rich organs such as the liver and kidneys (Bangma et al., 2022; Savoca and Pace, 2021). Other authors, such as Hernandez et al. (2022) and Xia et al. (2013), have demonstrated that the presence of proteins in solution can have a negative impact on bioavailable concentrations and absorption rates of dissolved PFOA in planktonic crustaceans, such as *D. magna*.

Currently, no treatment technology is suitable for large-scale application in addressing PFAS contaminations. Industrial and municipal wastewater treatment plants (WWTPs) are the main point sources of PFASs entering natural environments (Thompson et al., 2022). On the other hand, it has been observed that several PFASs, including PFOA, can be adsorbed by biological aggregates during activated sludge treatment within WWTPs (Zhou et al., 2024). Studies of these sludges have shown that the protein content of extracellular polymeric substances (EPSs) plays an important role in the sludge's ability to adsorb PFASs (Gravesen et al., 2023). Within the complex structure of these sludges, Yan et al. (2021) demonstrated that aromatic compounds, such as tryptophan (Trp), were able to bind by hydrophobic interactions to PFOA within EPSs. Thus, the adsorption process is a key step in both toxicity mechanisms and the treatment of PFAS contamination (Hernandez et al., 2022).

However, few studies have explored the individual contribution of amino acids, such as Trp, in attenuating the toxicological effects of PFOA. In order to provide an understanding of the behavior between Trp and PFOA, this study assessed the influence of L-Trp on the toxicological effect of PFOA in *D. magna*, demonstrated the formation of a Trp–PFOA complex, and investigated the structure of the complex.

2. Materials and méthodes

2.1. Chemicals

Perfluorooctanoic acid (PFOA; $C_8HF_{15}O_2$; CAS No. 335-67-1; ≥95%) and L-tryptophan (L-Trp; $C_{11}H_{12}N_2O_2$; CAS No. 73-22-3; ≥98%) were purchased from *MilliporeSigma Canada Ltd.* (Etobicoke, ON). Experimental concentration ranges were prepared immediately prior to use by diluting the stock solutions with *D. magna* culture medium (consisting of 102 $mg{\cdot}L^{-1}$ $NaHCO_3$, 4.25 $mg{\cdot}L^{-1}$ KCl, 63.75 $mg{\cdot}L^{-1}$ $MgSO_4$, 63.75 $mg{\cdot}L^{-1}$ $CaSO4{\cdot}2H_2O$ and 2 $\mu g{\cdot}L^{-1}$ SeO_2) reconstituted and aerated from NanoPure water (LEEQ, 2023).

2.2. Test organism and culture conditions

The *D. magna* strain used in this research was provided by the Ecotoxicology Department of Environment and Climate Change Canada's (ECCC) *Quebec Laboratory for Environmental Testing* (LEEQ, 2023). Experimental rearing cycles were conducted in reconstituted water enriched with vitamin B_{12} to 100 $\mu L{\cdot}L^{-1}$ and maintained at 20 ± 1 °C. A 16-h photoperiod was applied, with light intensity ranging from 600 to 800 lx at the water surface. The cultured *D. magna* were fed a fresh, laboratory-prepared algal mix of *Ankistrodesmus* sp. and *Raphidocelis subcapitata*, sourced from *Merlan Scientific* (Toronto, ON). Water quality parameters, including hardness (80–100 $mg\text{-}CaCO_3{\cdot}L^{-1}$), alkalinity, pH (6.8–8.5), conductivity, temperature, and dissolved oxygen, were monitored using standard methods (APHA, 2017). No males were observed during incubation. Each culture batch was used for a maximum of five weeks. At the start of the test, neonates (12–24 h old) from the third or later clutches were randomly selected.

2.3. Quality assurance and quality control

The physicochemical characteristics of the treatment and control media were analyzed before and after treatment; no parameters were measured outside the organism's tolerance limits, in accordance with OECD recommendations (OECD, 2012). No mortality or immobility was observed in *D. magna* during blank experiments. Sodium chloride (NaCl) was used as a reference toxicant in a sensitivity test in accordance with ECCC recommendations. All sensitivity test results were evaluated within the lower and upper warning limits, which were 5.06 $mg\text{-}NaCl{\cdot}L^{-1}$ and 6.01 $mg\text{-}NaCl{\cdot}L^{-1}$, respectively (Cowgill and Milazzo, 1991). Similarly, no significant differences ($p > 0.9999$) were observed in the sensitivity of different generations of *D. magna*. The correlation coefficients (R^2) of the experimental reference curves were greater than 0.99, and their repeatability was confirmed before each series of determinations.

2.4. Acute toxicity tests on D. magna

Experimental testing followed the guidelines of ECCC standard method LB-DAP-9 and the *International Organization for Standardization* standard ISO 6341:2012 (ISO, 2012; LEEQ, 2023). The experimental range of concentration levels in the acute toxicity tests was chosen to produce at least three observed effect percentages between 10% and 90%, based on preliminary test results. An appropriate dilution factor (f) of 0.72 was chosen (Yang et al., 2019). Five PFOA concentrations (80, 112, 156, 216, and 300 $mg{\cdot}L^{-1}$) were selected to establish the first LC_{50} – 48h (mortality) and EC_{50} - 48h (immobility) values. Toxicity tests were conducted at a temperature of 20 ± 2 °C with a photoperiod of 16 h at a light intensity of 700 lx and a dark cycle of 8 h. Blank *D. magna* culture medium was used as a control. Toxicity tests were carried out in six replicates with ten organisms per replicate.

A second series of tests was carried out with the same experimental range to assess the influence of L-Trp on PFOA toxicity. Each sample was prepared with reconstituted culture water enriched with L-Trp at 14.8, 74 and 148$mg{\cdot}L^{-1}$. A control group was set up to verify the absence of

any effect due to the presence of the amino acid, and a blank test without the addition of PFOA and amino acid was also conducted. The distinction between the two measurements was made when assessing immobility and mortality status after 48 h, and toxicity was expressed as percentage effect and mortality. In detail, test *D. magna* exhibiting abnormal movements (paralyzed limbs, inability to swim, missing reflexes) compared to control groups after repeated agitation of the medium were classified as immobile. Subsequently, *D. magna* were studied using a binocular microscope and classified as dead if no heartbeat could be detected within 15 s of agitation.

2.5. Analytical methods

2.5.1. Fluorescence quenching charaterization

The interactions between L-Trp and PFOA were studied by analyzing the fluorescence quenching of L-Trp using a Cary Eclipse fluorescence spectrometer (Argilent, USA). Scanning was performed at an excitation wavelengths from 200 to 400 nm with 2 nm increments, and emission was detected at a wavelength from 305 to 600 nm. Maximum study intensities were detected at 300 nm and 362 nm for excitation and emission, respectively.

Fluorescence quenching was analyzed quantitatively using the Stern-Volmer equation (Lakowicz, 2006):

$$F_0 / F = 1 + K_{SV}[Q] = 1 + K_q \tau_0 [Q] \quad (1)$$

Where, F_0 and F are the fluorescence intensities in the absence and presence of a quencher;

τ_0 is the average lifetime of the fluorophore in the absence of a quencher, equal to 10^{-8} s;

$[Q]$ is the quencher concentration (mol·L^{-1});

K_{SV} is the Stern-Volmer quenching constant (L·mol^{-1});

K_q is the biomolecule quenching rate constant (L·mol^{-1}·s^{-1}).

To gain a deeper understanding of extinction mechanisms, the results were adjusted using the modified Stern-Volmer equation (Lakowicz, 2006):

$$\frac{F_0}{F_0 - F} = \frac{1}{f_a K_a [Q]} + 1 \Big/ f_a \quad (2)$$

Where, F_0 and F are the fluorescence intensities in the absence and presence of a quencher;

f_a represents the fraction of accessible fluorophores;

K_a is the effective quenching constant for the accessible fluorophores;

$[Q]$ is the quencher concentration (mol·L^{-1}).

Finally, for a static quenching mechanism involving binding, where fluorescence quenching results from the formation of a complex between a fluorophore and a quencher, the equilibrium between the free molecule and the bound molecule can be described by the modified Hill equation (Wei et al., 2015):

$$Log \frac{F_0 - F}{F} = Log\, K_b + nLog[Q] \quad (3)$$

Where, F_0 and F are the fluorescence intensities in the absence and presence of a quencher;

K_b is the binding constant;

n is the Hill coefficient;

$[Q]$ is the quencher concentration (mol·L^{-1}).

2.5.2. Thermodynamic charaterization of th Trp–PFOA bond

To determine the nature of the interactions between L-Trp and PFOA, thermodynamic parameters such as the Gibbs free enthalpy variation (ΔG), enthalpy change (ΔH) and entropy change (ΔS) were calculated. When temperature variations are minimal, the enthalpy (H) of a system remains approximately constant, allowing the application of the following standard thermodynamic equations:

$$Ln\, K = -\Delta H/RT + \Delta S/R \quad (4)$$

Where, R is the gas constant (8314 J mol^{-1}·K^{-1});

T is the absolute temperature (K);

K is analogous to the binding constant K_b at the same temperature;

ΔH is the enthalpy change (kJ·mol^{-1});

ΔS is the entropy change (J·mol^{-1}·K^{-1}).

$$\Delta G = \Delta H - T\Delta S \quad (5)$$

Where, T is the absolute temperature (K);

ΔG is the Gibbs free energy change (kJ·mol^{-1});

ΔH is the enthalpy change (kJ·mol^{-1});

ΔS is the entropy change (J·mol^{-1}·K^{-1}).

2.5.3. Fourier transform infrared (FTIR) analysis

The bonds involved in the Trp-PFOA complex were studied using a Fourier transform infrared spectrometer (PerkinElmer, USA). The complex was formed in solution by adding L-Trp after total dissolution of PFOA in *D. magna* culture medium, then frozen and recovered as a powder by freeze-drying prior to analysis. Samples were analyzed at a resolution of 4 cm^{-1} over a range of 400 to 4000 cm^{-1} in transmittance mode.

2.6. Statistical analysis

The concentrations of chemical species that caused a 50% observed effect in *D. magna* were calculated using the Hill model with 95% confidence limits, employing the RegTox macro version 7.1.2 (Vindimian et al., 1983). A one-way analysis of variance (ANOVA), followed by a Tukey's post-hoc test was applied to the data to assess significant differences between treatments and controls using GraphPad Prism software version 10.2.2 for Windows (GraphPad Software, San Diego, CA, USA, http://www.graphpad.com). Results for each treatment were presented as means with the associated 95% confidence intervals (CIs) and coefficients of determination (R^2). All differences were considered significant at $p < 0.05$.

3. Results and discussion

3.1. Acute toxicity of test chemicals

Concentration-response relationships were established for molar ratios (*Trp:PFOA*) of *0:1*, *1:10*, *1:2,* and *1:1*, from which LC_{50} – 48h and EC_{50} – 48h values were estimated. The LC_{50} – 48h values for these ratios were 137 ± 24 mg·L^{-1}, 358 ± 65 mg·L^{-1}, 964 ± 491 mg·L^{-1}, and 707 ± 147 mg·L^{-1}, respectively (Fig. 1a). The corresponding EC_{50} – 48h values were 109 ± 16 mg·L^{-1}, 303 ± 44 mg·L^{-1}, 614 ± 99 mg·L^{-1}, and 418 ± 62 mg·L^{-1}, respectively (Fig. 1b). Toxicity tests revealed that all three treatments (*0.1:1*, *0.5:1,* and *1:1)* resulted in a significant reduction in both mortality ($p = 0.0036$, $p < 0.0001$, and $p < 0.0001$) and immobility ($p = 0.0029$, $p < 0.0001$, and $p = 0.0001$). However, the experimental data did not demonstrate significant differences between the treatments.

The results of the acute toxicity analyses showed that L-Trp led to a reduction in PFOA toxicity. After 48 h exposure, the effect of L-Trp on mortality and immobility in *D. magna* was directly correlated with the concentration of the amino acid. Concentration-response relationships show that the interaction between L-Trp and PFOA is neither linear nor directly dose-dependent. Instead, they suggest the presence of an optimal molar ratio of around 1:2 (Trp:PFOA), to effectively reduce PFOA toxicity. Beyond this ratio, the effectiveness of L-Trp in attenuating PFOA toxicity no longer increases monotonically, probably due to the formation of transient interactions, competitive interactions, or even a limit in reaction yield. Similar results have also been observed at

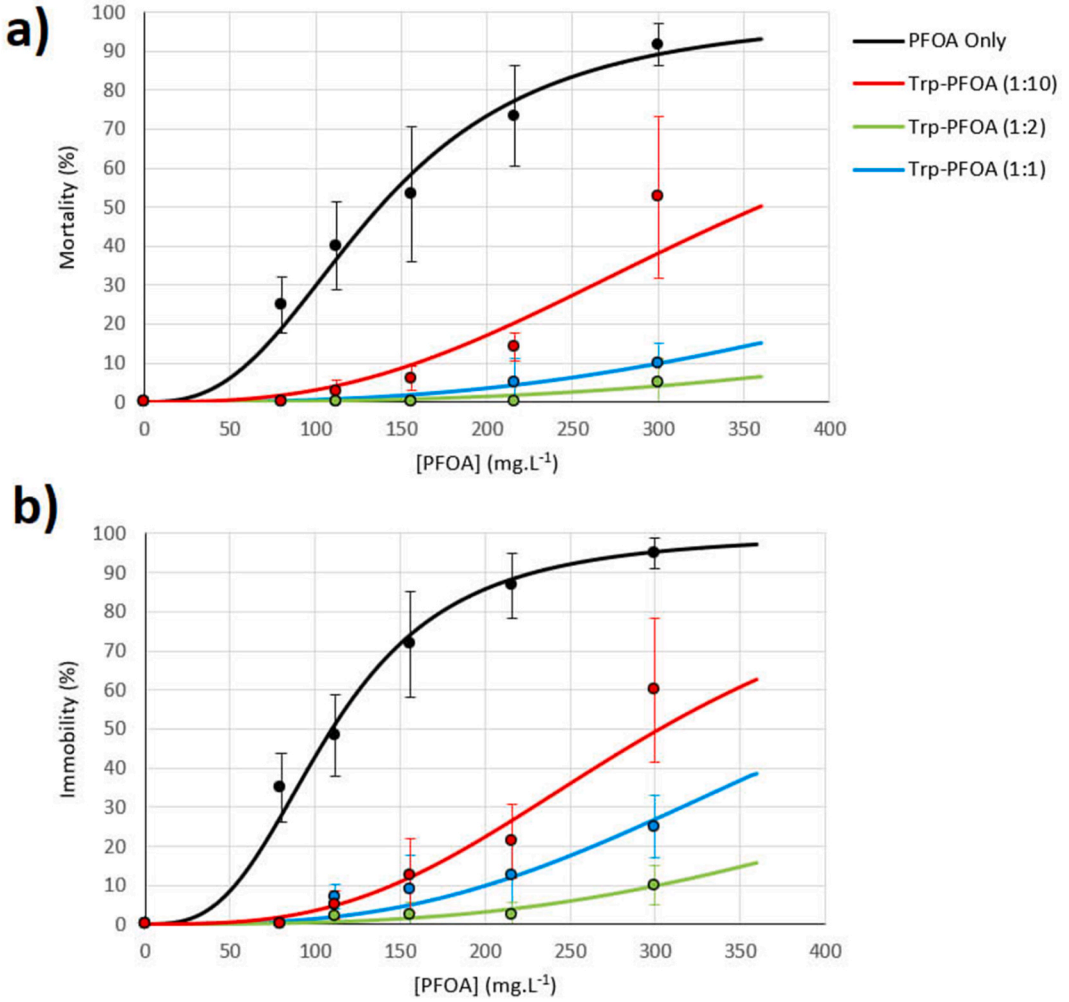

Fig. 1. Concentration-response relationships of *D. magna* after 48 h exposure to concentration ratios (*Trp:PFOA*) of *0:1, 1:10, 1:2* and *1:1*, a) for mortality observation and b) for immobility observation. All relationships differed significantly ($p < 0.005$) from the reference relationship.

protein level from the point of view of PFOA bioaccumulation in *D. magna*, with higher PFOA body loading rates in *D. magna* at the highest protein concentrations (Xia et al., 2013). One explanation for this phenomenon is the simultaneous influence of protein compounds on PFASs uptake and elimination rates in *D. magna* (Dai et al., 2013). These results suggest that L-Trp is able to bind to PFOA to form a larger carbon entity. This interaction would result in modified PFOA uptake and removal via steric exclusion and electrostatic repulsion mechanisms (Leung et al., 2023), as well as possible partial PFOA inactivation.

This hypothesis is supported by a specific optimal stoichiometric equilibrium between L-Trp and PFOA at a ratio of 1:2, where each L-Trp molecule seems to be able to bind to two PFOA molecules. This binding could occur either independently or through layered structuring, similar to what is observed in some biological and polymeric systems (Alberts et al., 2002; Kravchenko et al., 2021). However, such organization could theoretically be sensitive to variations in the environment (e.g., concentration, temperature), as shown by the increase in toxicity observed at the 1:1 ratio.

3.2. Fluorescences interactions between L-Trp and PFOA

The presence of an indole ring in the L-Trp structure confers spectroscopic properties of UV absorption at approximately 280 nm and fluorescence emission at approximately 350 nm. As shown in Fig. 2a, a slight red shift was observed for the emission value at 362 nm. This can be explained by the sensitivity of L-Trp's photophysical properties to its microenvironment, notably due to hydrogen bonds characterized by a red shift with increasing polarity (Uriza-Prias et al., 2022).

As shown in Fig. 2a, emission intensities progressively decreased with increasing PFOA dosage. This indicates that PFOA was able to interact with the indole group of L-Trp. These observations confirm the existence of such interactions as reported in the literature (Jiao et al., 2022; Yan et al., 2021). Similarly, increasing the molar ratio led to decreases of 13%, 24%, 33%, and 37%, respectively, compared with the reference intensity. Such non-uniform decreases suggest complex binding dynamics, potentially involving multiple binding sites and variable affinity, where the interaction does not reach full saturation. A higher molar ratio of L-Trp could induce the formation of less stable or transient complexes and fluctuating bioavailability of free PFOA, contributing to the observed non-monotonic effects on *D. magna* mortality and immobility. Consequently, the quenching behavior indicates that fluorescence quenching is not linearly correlated with PFOA's toxic effect, suggesting that free PFOA exhibits erratic toxicological patterns in the presence of the amino acid. In addition, increasing the PFOA dosage led to a slight shift in the wavelength of the blue emission peak from 362 to 356 nm, indicating increased hydrophobicity around L-Trp (Uriza-Prias et al., 2022).

The fluorescence quenching process is generally associated with two underlying mechanisms: dynamic quenching and static quenching. Dynamic quenching occurs when there is a collision between the fluorophore and quencher in the excited state, while static quenching results from the formation of a non-fluorescent complex between the fluo-

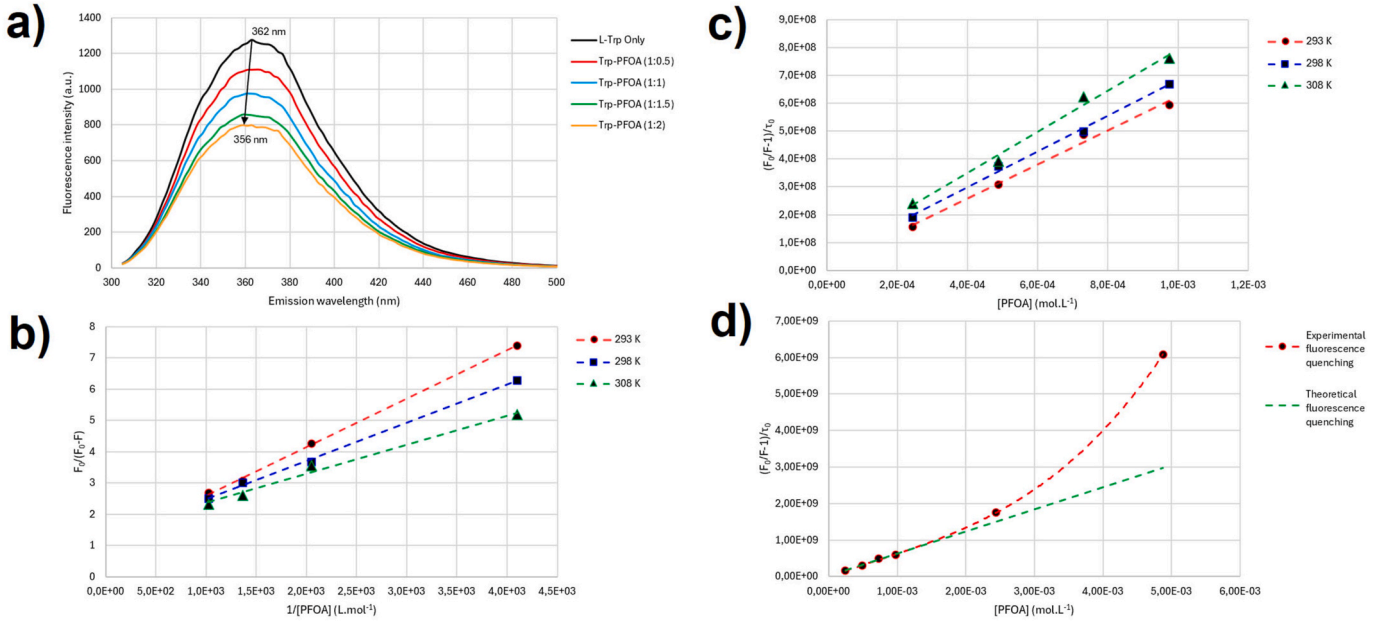

Fig. 2. (a) Emission spectrum of the interaction between L-Trp and PFOA at 293 K; (b) Stern-Volmer plot of L-Trp as a function of PFOA dosage at 293, 298 and 308 K; (c) Modified Stern-Volmer diagram for L-Trp extinction in the presence of PFOA at 293, 298 and 308 K; (d) Comparison of theoretical and experimental Stern-Volmer plots for an extended concentration range at 293 K.

rophore and quencher prior to excitation under the influence of external forces (Fossum et al., 2023). To understand the mechanism involved in L-Trp fluorescence quenching, the Stren-Volmer equation (Eq. (1)) was used to fit data at 293, 298 and 308 K (Fig. 2b). This temperature range was chosen to minimize enthalpy variations and for reasons of environmental relevance. As shown in Table 1, modeling of the fluorescence data showed good correlation with the Stren-Volmer equation. The biomolecule quenching rate constant (K_q), which reflect the impact of collisions or molecular diffusion on the fluorescence decay rate, were all evaluated above the maximum diffusive collision extinction rate constant (2.00×10^{10} L·mol^{-1}·s^{-1}) (Fossum et al., 2023). This observation suggests that a static quenching mechanism was involved in the interactions between L-Trp and PFOA. However, Table 1 shows that K_q values increased with temperature, suggesting the existence of a dynamic quenching mechanism (Wu et al., 2020). Thus, the observed decrease in fluorescence would be due to a combination of a dynamic and a static quenching mechanism.

To enable a better understanding of the extinction mechanisms, the data were subjected to a fit using the modified Stern-Volmer equation (Eq. (2)). Here, since L-Trp is free in solution, it offers equal opportunities for interactions with other molecules, so $f_a = 1$ (Wei et al., 2015). As shown in Fig. 2c, modelling of the fluorescence data indicated a good correlation with the modified Stren-Volmer equation. The upward trend in K_a confirms the existence of a dynamic quenching mode. A rise in temperature leads to faster diffusion and a higher proportion of collisional extinction; but also to the dissociation of weakly bound complexes and therefore comparatively smaller amounts of static extinction (Fossum et al., 2023). Consequently, the fluorescence quenching involved in interactions between L-Trp and PFOA is dominated by a dynamic quenching mode.

In order to verify the existence or otherwise of a static extinction mode during interactions between L-Trp and PFOA, the concentration range studied was extended to two extreme concentrations at 293 K (Fig. 2d). As shown in Fig. 2d, the experimental Stern-Volmer plot diverged significantly from the theoretical linear plot of single-mode fluorescence quenching. In addition, the experimental Stern-Volmer plot gradually showed an upward curvature, typical of combined extinctions (Wei et al., 2015). Thus, these observations confirm that both modes of fluorescence quenching occurred simultaneously between L-Trp and PFOA in this study.

Table 1
Stern-Volmer quenching constant (K_{SV}), biomolecule quenching rate constant (K_q) and effective quenching constant (K_a) for the interaction between L-Trp and PFOA according to the Stern-Volmer equations at 293, 298 and 308 K. R^2 is the correlation coefficient.

T (K)	K_{SV} (L·mol^{-1})	K_q (L·mol^{-1}·s^{-1})	R^2	K_a (L·mol^{-1})	R^2
293	6.11×10^4	6.11×10^{12}	0.992	6.25×10^2	0.999
298	6.40×10^4	6.40×10^{12}	0.995	8.33×10^2	0.998
308	7.38×10^4	7.38×10^{12}	0.991	1.11×10^3	0.987

3.3. Nature of the binding mode and thermodynamic parameters of L-Trp/PFOA complex

From Fig. 3a, the correlation coefficients (R^2) for the binding constants were greater than 0.98 (Table 2), indicating that the interaction of L-Trp with PFOA fit well with the site-binding model described by equation (Eq. (3)). According to Equation (3), the Hill coefficients (n) were close to 1 (Table 2). This observation confirms that the indole ring of L-Trp constitutes a binding site for PFOA molecules. Furthermore, n values very close to 1 indicate independent, even slightly non-cooperative binding (Lakowicz, 2006). In the case of toxicity tests in *D. magna* at 293 K, this supports the hypothesis that L-Trp is capable of forming independent bonds on either side of the indole plane with PFOA molecules.

From Fig. 3b, the Van't Hoff plot showed that the enthalpy of the system remained relatively constant. Here, $\Delta G < 0$ indicates that the reaction between L-Trp and PFOA is spontaneous between 293 and 308 K. Furthermore, as both ΔH and ΔS are below zero, this suggests that van der Waals interactions and hydrogen bonds play a major role in the equilibrium of the Trp–PFOA complex (Chen et al., 2015). Thus, contrary to the observations of Tang et al. (2022) and Yan et al. (2021), electrostatic forces and the hydrophobic effect would be only secondary forces in stabilizing the complex. All these non-covalent interactions, known for their impact on the properties, behavior and environmental fate of many pollutants, provide a plausible explanation for the

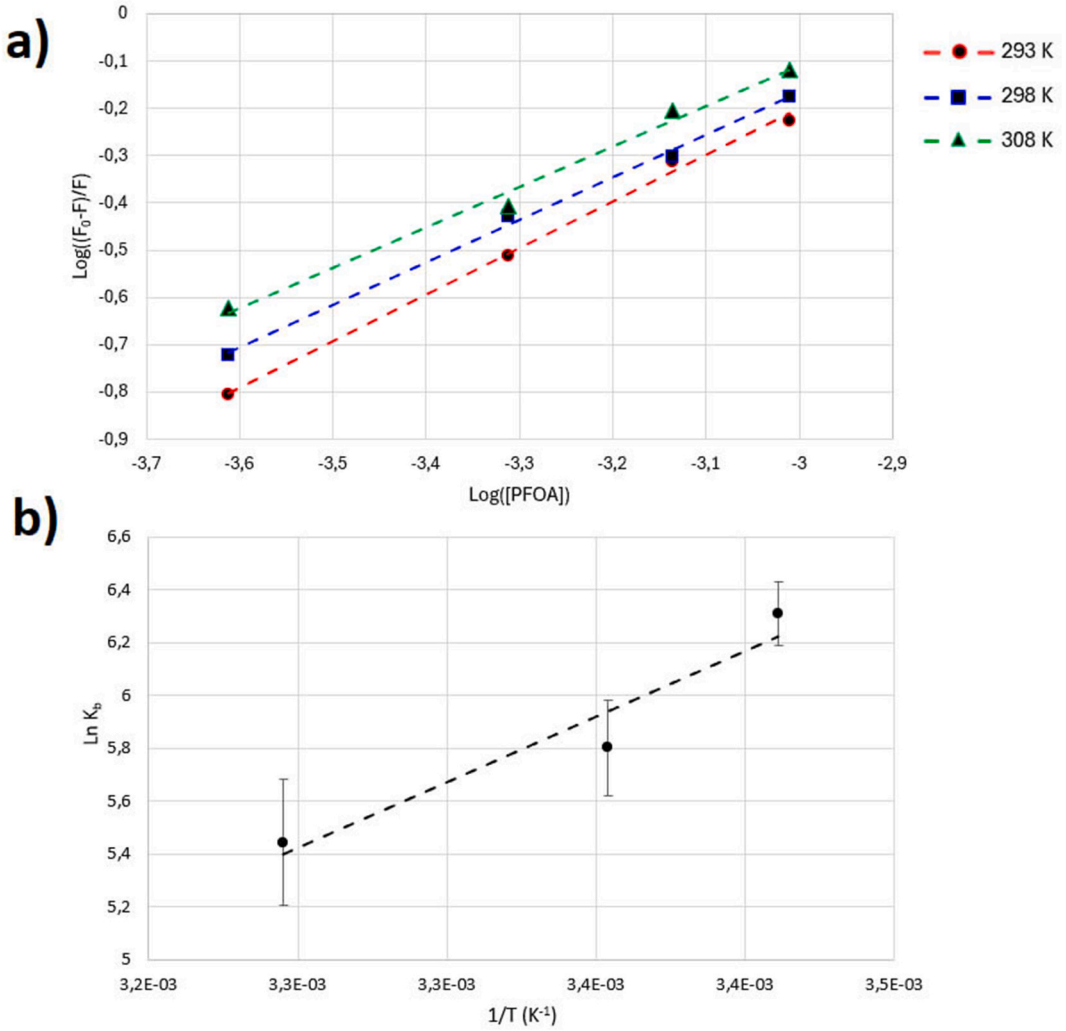

Fig. 3. (a) Modified Hill diagram for L-Trp binding to PFOA at 293, 298 and 308 K; (b) Van't Hoff plot of ln K_b versus 1/T for Trp binding to PFOA.

Table 2
Binding parameters, including binding constant (K_b), Hill coefficient (n) and relative thermodynamic parameters for the interaction between L-Trp and PFOA at 293, 298 and 308 K. R^2 is the correlation coefficient.

T (K)	K_b (L·mol^{-1})	n	R^2	ΔH (kJ·mol^{-1})	ΔS (J·mol^{-1}·K^{-1})	ΔG (kJ·mol^{-1})	R^2
293	5.01×10^2	0.983	0.9966	−46.19	−88.12	−20.37	0.925
298	3.16×10^2	0.897	0.9843			−19.93	
308	2.51×10^2	0.855	0.9850			−19.05	

reduction in toxicity observed in *D. magna* (Fang et al., 2015; Kern et al., 2022).

Drawing an analogy from the medical field, L-Trp could constitute a micellar effect similar to polymeric micelles recognized as scalable drug delivery vehicles that reduce toxicity and improve therapeutic efficacy of free drugs depending on their size, biocompatibility, thermodynamic stability, and kinetics (Lin et al., 2021). In this way, L-Trp is likely to have a direct effect on the bioavailability of free PFOA, or even influence its behavior and distribution in the body. However, further investigations are needed to establish the actual behavior of PFOA in the presence of amino acids, such as L-Trp, or even at the protein level.

3.4. Identification of binding groups in L-Trp/PFOA complex

As shown in Fig. 4, the characteristic absorption bands of both molecules shifted in the molar mixtures, confirming an interaction between L-Trp and PFOA. Specifically, the intensity of L-Trp's characteristic bands decreased with increasing PFOA dosage. The absorption bands associated with carbonyl groups shifted from 1755 cm^{-1} (C═O stretching) to 1721 cm^{-1}, and from 1661 cm^{-1} (antisymmetric stretching of –COO$^-$ associated with H₂N–H antisymmetric bending modes) to 1633 cm^{-1}, suggesting their involvement in hydrogen bonding. Conversely, the decrease and shift of the characteristic aromatic C═C bands towards higher frequencies, coupled with the variation and disappearance of C–H and =C–N– bands, indicate a local reduction in hydrogen bonding. This phenomenon supports the hypothesis that PFOA is attracted to the indole group of L-Trp through hydrophobic effects (Yan et al., 2021). The reduced intensity of the band at 3402 cm^{-1} (–N–H indole stretching) and the disappearance of the band at 1582 cm^{-1} (H_2N–H antisymmetric bending) may result from electrostatic attraction between the protonated amine of L-Trp and the negatively charged carboxylic group of PFOA (Yan et al., 2021). Thus, in addition

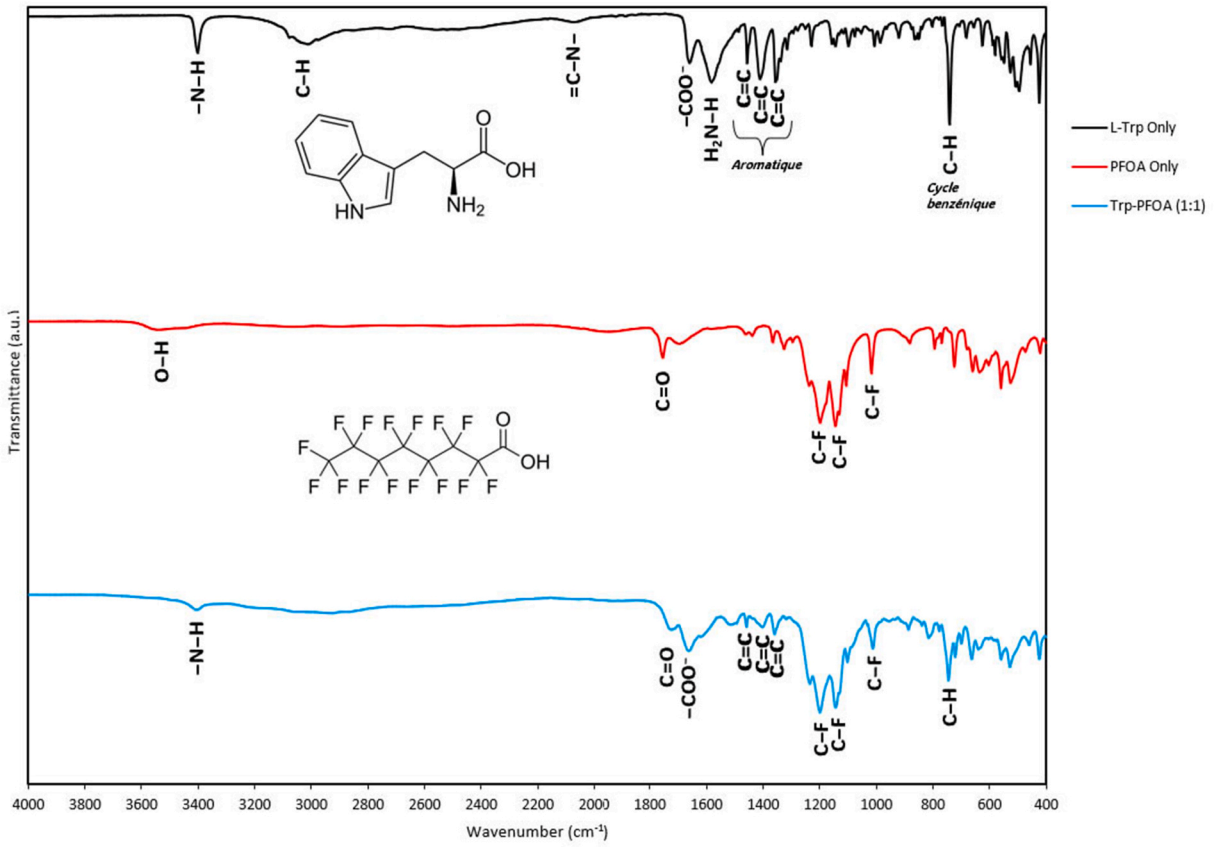

Fig. 4. FTIR spectra of pure L-Trp, pure PFOA and a Trp-PFOA mixture (1:1) recovered as powders by freeze-drying.

to the previously discussed interactions, the amine group in L-Trp provides an additional interaction site for PFOA through electrostatic forces.

3.5. Implications of the complexation mechanism

The specific features of the Trp–PFOA complex demonstrate the existence of physicochemical conditions for attenuating the toxicological effects of PFOA. The optimal stoichiometry at a 1:2 ratio reveals not only a particular affinity between L-Trp and PFOA but also the involvement of underlying molecular mechanisms influencing the biological response. This specific interaction indicates that the indole ring acts as a preferred binding site for PFOA, leading to particular toxicological profiles that cannot be predicted based solely on total concentrations. The toxicological responses observed highlight the impact of complexation on PFOA bioavailability and reflect its influence on toxicokinetic parameters. Thus, this phenomenon introduces new variability in PFOA toxicity, strongly influenced by the dynamic equilibrium between bound and free forms.

Previous studies have also observed similar interactions between the indole ring and other PFASs (Alesio and Bothun, 2024; Chen et al., 2024; Jin et al., 2022), suggesting that this binding is a common feature that may more broadly influence PFAS behavior. This specificity persists even in more complex physicochemical environments (Tang et al., 2022; Yan et al., 2021), indicating that molecules containing indolic structures play a significant role in modulating the environmental fate and toxicity of PFASs. Notably, Jin et al. (2022) demonstrated that the formulation of indolic derivatives enabled high adsorption and even defluorination of PFOA and PFOS under certain conditions.

Furthermore, the non-covalent nature of the forces involved in complexation, as well as their dependence on environmental conditions such as temperature and molecule concentration, suggest that the reaction is reversible. This reversibility is interesting from a toxicity standpoint. Indeed, the ubiquity of compounds containing indole nuclei in aquatic environments and living organisms could be an underestimated modulating factor in PFOA transport, accumulation, and bioavailability. For example, it has been observed that increasing temperature affects the bioconcentration and bioaccumulation of PFASs by releasing contaminants trapped in sediments, increasing their uptake rates in environmental organisms (Wang et al., 2023).

This reversibility of the reaction with the indole ring of L-Trp also raises questions about the effectiveness of biological treatments. The sorption capacity of PFASs by activated sludge relies on their protein content (Arvaniti et al., 2014; Behnami et al., 2024; Yan et al., 2021), and aromatic compounds, such as tryptophan and tyrosine (Tang et al., 2022; Yan et al., 2021; Zhang et al., 2023). Consequently, the presence of labile bonds, as illustrated here, could lead to the release of adsorbed PFASs into the natural environment during washing or incineration processes.

The observations of this study, combined with those of previous research, underline the importance of the indole group and analogous molecules in binding to PFASs. This dynamic opens up new perspectives for understanding the mechanisms of interaction between PFASs and biological compounds, as well as for developing more effective treatment strategies and environmental regulations. Future research should further explore these interactions, particularly in complex environments and with other indole compounds, to better assess their impact on the toxicity and environmental fate of PFASs.

4. Conclusion

This study demonstrates that L-Trp significantly reduces mortality and acute immobility in *D. magna* through the formation of a Trp–PFOA complex. Bioassays demonstrated the existence of a Trp:PFOA molar

ratio around 1:2 for optimal attenuation of toxicological effects, indicating L-Trp's potential to react with two PFOA molecules. Fluorescence quenching analyses revealed that non-covalent interactions, particularly van der Waals forces and hydrogen bonds, play a central role in the formation of the Trp–PFOA complex. Determination of thermodynamic parameters further supported these findings, and FTIR analysis confirmed the presence of hydrophobic and electrostatic interactions within the complex. The presence of such interactions implies reversibility of the reaction. Consequently, the reversibility of Trp–PFOA complexes could explain the erratic results of research into PFAS toxicity. Similarly, biological treatment processes for PFAS contamination based on this mechanism are likely to be affected by this reversibility. Moreover, the potential for reversible complexation with biomolecules in the natural environment raises concerns about current PFAS regulations. Future research should explore the behavior of homologous PFASs in relation to amino acids and proteins to better understand these interactions and their implications.

CRediT authorship contribution statement

Mathieu Verhille: Writing – original draft, Methodology, Investigation, Formal analysis, Conceptualization. **Robert Hausler:** Writing – review & editing, Validation.

Declaration of competing interest

The authors declare that they have no known competing financial interests or personal relationships that could have appeared to influence the work reported in this paper.

Data availability

Data will be made available on request.

References

Alberts, B., Johnson, A., Lewis, J., Raff, M., Roberts, K., Walter, P., 2002. The lipid bilayer. In: Molecular Biology of the Cell, fourth ed. Garland Science.

Alesio, J., Bothun, G.D., 2024. Differential scanning fluorimetry to assess PFAS binding to bovine serum albumin protein. Sci. Rep. 14, 6501. https://doi.org/10.1038/s41598-024-57140-9.

Ankley, G.T., Cureton, P., Hoke, R.A., Houde, M., Kumar, A., Kurias, J., Lanno, R., McCarthy, C., Newsted, J., Salice, C.J., Sample, B.E., Sepúlveda, M.S., Steevens, J., Valsecchi, S., 2021. Assessing the ecological risks of per- and polyfluoroalkyl substances: current state-of-the science and a proposed path forward. Environ. Toxicol. Chem. 40, 564–605. https://doi.org/10.1002/etc.4869.

APHA, 2017. Standard Methods for the Examination of Water, 23 éd. American Public Health Association, Washington, DC.

Arvaniti, O.S., Andersen, H.R., Thomaidis, N.S., Stasinakis, A.S., 2014. Sorption of Perfluorinated Compounds onto different types of sewage sludge and assessment of its importance during wastewater treatment. Chemosphere 111, 405–411. https://doi.org/10.1016/j.chemosphere.2014.03.087.

Bangma, J., Guillette, T.C., Bommarito, P.A., Ng, C., Reiner, J.L., Lindstrom, A.B., Strynar, M.J., 2022. Understanding the dynamics of physiological changes, protein expression, and PFAS in wildlife. Environ. Int. 159, 107037. https://doi.org/10.1016/j.envint.2021.107037.

Behnami, A., Zoroufchi Benis, K., Pourakbar, M., Yeganeh, M., Esrafili, A., Gholami, M., 2024. Biosolids, an important route for transporting poly- and perfluoroalkyl substances from wastewater treatment plants into the environment: a systematic review. Sci. Total Environ. 925, 171559. https://doi.org/10.1016/j.scitotenv.2024.171559.

Bertin, D., Ferrari, B.J.D., Labadie, P., Sapin, A., Garric, J., Budzinski, H., Houde, M., Babut, M., 2014. Bioaccumulation of perfluoroalkyl compounds in midge (Chironomus riparius) larvae exposed to sediment. Environ Pollut 189, 27–34. https://doi.org/10.1016/j.envpol.2014.02.018.

Chen, H., He, P., Rao, H., Wang, F., Liu, H., Yao, J., 2015. Systematic investigation of the toxic mechanism of PFOA and PFOS on bovine serum albumin by spectroscopic and molecular modeling. Chemosphere, Per- and Polyfluorinated Alkyl substances (PFASs) in materials, humans and the environment – current knowledge and scientific gaps 129, 217–224. https://doi.org/10.1016/j.chemosphere.2014.11.040.

Chen, Z., Dong, R., Wang, X., Huang, L., Qiu, L., Zhang, M., Mi, N., Xu, M., He, H., Gu, C., 2024. Efficient decomposition of perfluoroalkyl substances by low concentration indole: new insights into the molecular mechanisms. Environ. Sci. Technol. 58, 3530–3539. https://doi.org/10.1021/acs.est.3c08453.

Cowgill, U.M., Milazzo, D.P., 1991. Demographic effects of salinity, water hardness and carbonate alkalinity on Daphnia magna and Ceriodaphnia dubia. Arch. Hydrobiol. 122, 33–56.

Dai, Z., Xia, X., Guo, J., Jiang, X., 2013. Bioaccumulation and uptake routes of perfluoroalkyl acids in Daphnia magna. Chemosphere 90, 1589–1596. https://doi.org/10.1016/j.chemosphere.2012.08.026.

Death, C., Bell, C., Champness, D., Milne, C., Reichman, S., Hagen, T., 2021. *Per-* and polyfluoroalkyl substances (PFAS) in livestock and game species: a review. Sci. Total Environ. 774, 144795. https://doi.org/10.1016/j.scitotenv.2020.144795.

Du, D., Lu, Y., Zhou, Y., Li, Q., Zhang, M., Han, G., Cui, H., Jeppesen, E., 2021. Bioaccumulation, trophic transfer and biomagnification of perfluoroalkyl acids (PFAAs) in the marine food web of the South China Sea. J. Hazard Mater. 405, 124681. https://doi.org/10.1016/j.jhazmat.2020.124681.

Fang, W., Sheng, G.-P., Wang, L.-F., Ye, X.-D., Yu, H.-Q., 2015. Quantitative evaluation of noncovalent interactions between polyphosphate and dissolved humic acids in aqueous conditions. Environmental Pollution 207, 123–129. https://doi.org/10.1016/j.envpol.2015.09.001.

Fossum, C.J., Johnson, B.O.V., Golde, S.T., Kielman, A.J., Finke, B., Smith, M.A., Lowater, H.R., Laatsch, B.F., Bhattacharyya, S., Hati, S., 2023. Insights into the mechanism of tryptophan fluorescence quenching due to synthetic crowding agents: a combined experimental and computational study. ACS Omega 8, 44820–44830. https://doi.org/10.1021/acsomega.3c06006.

Gravesen, C.R., Lee, L.S., Choi, Y.J., Silveira, M.L., Judy, J.D., 2023. PFAS release from wastewater residuals as a function of composition and production practices. Environmental Pollution 322, 121167. https://doi.org/10.1016/j.envpol.2023.121167.

Hernandez, E.T., Koo, B., Sofen, L.E., Amin, R., Togashi, R.K., Lall, A.I., Gisch, D.J., Kern, B.J., Rickard, M.A., Francis, M.B., 2022. Proteins as adsorbents for PFAS removal from water. Environ. Sci.: Water Res. Technol. 8, 1188–1194. https://doi.org/10.1039/D1EW00501D.

ISO, 2012. Qualité de l'eau — Détermination de l'inhibition de la mobilité de Daphnia magna Straus (Cladocera, Crustacea) — Essai de toxicité aiguë.

Jiao, Y., Zou, M., Yang, X., Tsang, Y.F., Chen, H., 2022. Perfluorooctanoic acid triggers oxidative stress in anaerobic digestion of sewage sludge. J. Hazard Mater. 424, 127418. https://doi.org/10.1016/j.jhazmat.2021.127418.

Jin, X., Wang, Z., Hong, R., Chen, Z., Wu, B., Ding, S., Zhu, W., Lin, Y., Gu, C., 2022. Supramolecular assemblies of a newly developed indole derivative for selective adsorption and photo-destruction of perfluoroalkyl substances. Water Res. 225, 119147. https://doi.org/10.1016/j.watres.2022.119147.

Kang, J.S., Ahn, T.-G., Park, J.-W., 2019. Perfluorooctanoic acid (PFOA) and perfluooctane sulfonate (PFOS) induce different modes of action in reproduction to Japanese medaka (*Oryzias latipes*). J. Hazard Mater. 368, 97–103. https://doi.org/10.1016/j.jhazmat.2019.01.034.

Kern, M., Škulj, S., Rožman, M., 2022. Adsorption of a wide variety of antibiotics on graphene-based nanomaterials: a modelling study. Chemosphere 296, 134010. https://doi.org/10.1016/j.chemosphere.2022.134010.

Kravchenko, V.S., Abetz, V., Potemkin, I.I., 2021. Self-assembly of gradient copolymers in a selective solvent. New structures and comparison with diblock and statistical copolymers. Polymer 235, 124288. https://doi.org/10.1016/j.polymer.2021.124288.

Kwak, J.I., Lee, T.-Y., Seo, H., Kim, Dokyung, Kim, Dasom, Cui, R., An, Y.-J., 2020. Ecological risk assessment for perfluorooctanoic acid in soil using a species sensitivity approach. J. Hazard Mater. 382, 121150. https://doi.org/10.1016/j.jhazmat.2019.121150.

Lakowicz, J.R., 2006. Principles of Fluorescence Spectroscopy, third ed. 2006. Corr. 5th printing 2010 edition. Springer, New York.

Lau, C., 2015. Perfluorinated compounds: an overview. In: DeWitt, J.C. (Ed.), Toxicological Effects of Perfluoroalkyl and Polyfluoroalkyl Substances. Springer International Publishing, Cham, pp. 1–21. https://doi.org/10.1007/978-3-319-15518-0_1.

LEEQ, 2023. Acquisition, acclimatation et maintien de la culture de Daphnia magna (Protocole technique No. LB-DAC-8). Environnement et Changement climatique Canada, Canada.

Leung, S.C.E., Wanninayake, D., Chen, D., Nguyen, N.-T., Li, Q., 2023. Physicochemical properties and interactions of perfluoroalkyl substances (PFAS) - challenges and opportunities in sensing and remediation. Sci. Total Environ. 905, 166764. https://doi.org/10.1016/j.scitotenv.2023.166764.

Li, Y., Yao, J., Pan, Y., Dai, J., Tang, J., 2023. Trophic behaviors of PFOA and its alternatives perfluoroalkyl ether carboxylic acids (PFECAs) in a coastal food web. J. Hazard Mater. 452, 131353. https://doi.org/10.1016/j.jhazmat.2023.131353.

Lin, M., Dai, Y., Xia, F., Zhang, X., 2021. Advances in non-covalent crosslinked polymer micelles for biomedical applications. Mater. Sci. Eng. C 119, 111626. https://doi.org/10.1016/j.msec.2020.111626.

Manojkumar, Y., Pilli, S., Rao, P.V., Tyagi, R.D., 2023. Sources, occurrence and toxic effects of emerging per- and polyfluoroalkyl substances (PFAS). Neurotoxicol. Teratol. 97, 107174. https://doi.org/10.1016/j.ntt.2023.107174.

OECD, 2012. Daphnia Magna Acute Immobilisation Test and Reproduction Test, Guidelines for Testing of Chemicals.

Pan, Y., Zhang, H., Cui, Q., Sheng, N., Yeung, L.W.Y., Sun, Y., Guo, Y., Dai, J., 2018. Worldwide distribution of novel perfluoroether carboxylic and sulfonic acids in surface water. Environ. Sci. Technol. 52, 7621–7629. https://doi.org/10.1021/acs.est.8b00829.

Pérez, F., Nadal, M., Navarro-Ortega, A., Fàbrega, F., Domingo, J.L., Barceló, D., Farré, M., 2013. Accumulation of perfluoroalkyl substances in human tissues. Environ. Int. 59, 354–362. https://doi.org/10.1016/j.envint.2013.06.004.

Savoca, D., Pace, A., 2021. Bioaccumulation, biodistribution, toxicology and biomonitoring of organofluorine compounds in aquatic organisms. Int. J. Mol. Sci. 22, 6276. https://doi.org/10.3390/ijms22126276.

Steenland, K., Fletcher, T., Stein, C.R., Bartell, S.M., Darrow, L., Lopez-Espinosa, M.-J., Barry Ryan, P., Savitz, D.A., 2020. Review: evolution of evidence on PFOA and health following the assessments of the C8 Science Panel. Environ. Int. 145, 106125. https://doi.org/10.1016/j.envint.2020.106125.

Sunderland, E.M., Hu, X.C., Dassuncao, C., Tokranov, A.K., Wagner, C.C., Allen, J.G., 2019. A review of the pathways of human exposure to poly- and perfluoroalkyl substances (PFASs) and present understanding of health effects. J. Expo. Sci. Environ. Epidemiol. 29, 131–147. https://doi.org/10.1038/s41370-018-0094-1.

Tang, L., Su, C., Fan, C., Li, R., Wang, Y., Gao, S., Chen, M., 2022. Long-term effect of perfluorooctanoic acid on the anammox system based on metagenomics: performance, sludge characteristic and microbial community dynamic. Bioresour. Technol. 351, 127002. https://doi.org/10.1016/j.biortech.2022.127002.

Thompson, K.A., Mortazavian, S., Gonzalez, D.J., Bott, C., Hooper, J., Schaefer, C.E., Dickenson, E.R.V., 2022. Poly- and perfluoroalkyl substances in municipal wastewater treatment plants in the United States: seasonal patterns and meta-analysis of long-term trends and average concentrations. ACS EST Water 2, 690–700. https://doi.org/10.1021/acsestwater.1c00377.

Uriza-Prias, D.M., Méndez-Blas, A., Rivas-Silva, J.F., 2022. A study of the effects of the polarity of the solvents acetone and cyclohexane on the luminescent properties of tryptophan. Spectrochim. Acta Mol. Biomol. Spectrosc. 266, 120434. https://doi.org/10.1016/j.saa.2021.120434.

Vindimian, E., Robaut, C., Fillion, G., 1983. A method for cooperative or noncooperative binding studies using nonlinear regression analysis on a microcomputer. J. Appl. Biochem. 5, 261–268.

Wang, H., Hu, D., Wen, W., Lin, X., Xia, X., 2023. Warming affects bioconcentration and bioaccumulation of per- and polyfluoroalkyl substances by pelagic and benthic organisms in a water–sediment system. Environ. Sci. Technol. 57, 3612–3622. https://doi.org/10.1021/acs.est.2c07631.

Wei, D., Wang, B., Ngo, H.H., Guo, W., Han, F., Wang, X., Du, B., Wei, Q., 2015. Role of extracellular polymeric substances in biosorption of dye wastewater using aerobic granular sludge. Bioresour. Technol. 185, 14–20. https://doi.org/10.1016/j.biortech.2015.02.084.

Wen, B., Wu, Y., Zhang, H., Liu, Y., Hu, X., Huang, H., Zhang, S., 2016. The roles of protein and lipid in the accumulation and distribution of perfluorooctane sulfonate (PFOS) and perfluorooctanoate (PFOA) in plants grown in biosolids-amended soils. Environmental Pollution 216, 682–688. https://doi.org/10.1016/j.envpol.2016.06.032.

Wu, F., Song, X.-M., Qiu, Y.-L., Zheng, H.-Q., Hu, F.-L., Li, H.-L., 2020. Unique dynamic mode between Artepillin C and human serum albumin implies the characteristics of Brazilian green propolis representative bioactive component. Sci. Rep. 10, 17277. https://doi.org/10.1038/s41598-020-74197-4.

Xia, X., Rabearisoa, A.H., Jiang, X., Dai, Z., 2013. Bioaccumulation of perfluoroalkyl substances by Daphnia magna in water with different types and concentrations of protein. Environ. Sci. Technol. 47, 10955–10963. https://doi.org/10.1021/es401442y.

Yan, W., Qian, T., Zhang, L., Wang, L., Zhou, Y., 2021. Interaction of perfluorooctanoic acid with extracellular polymeric substances - role of protein. J. Hazard Mater. 401, 123381. https://doi.org/10.1016/j.jhazmat.2020.123381.

Yang, H.-B., Zhao, Y.-Z., Tang, Y., Gong, H.-Q., Guo, F., Sun, W.-H., Liu, S.-S., Tan, H., Chen, F., 2019. Antioxidant defence system is responsible for the toxicological interactions of mixtures: a case study on PFOS and PFOA in Daphnia magna. Sci. Total Environ. 667, 435–443. https://doi.org/10.1016/j.scitotenv.2019.02.418.

Zhang, S., Zhang, H., Feng, Y., Maddela, N.R., Li, S., Zhang, L., 2023. Insights into the responses of the partial denitrification process to elevated perfluorooctanoic acid stress: performance, EPS characteristic and microbial community. Water 15, 2977. https://doi.org/10.3390/w15162977.

Zhao, L., Teng, M., Zhao, X., Li, Y., Sun, J., Zhao, W., Ruan, Y., Leung, K.M.Y., Wu, F., 2023. Insight into the binding model of per- and polyfluoroalkyl substances to proteins and membranes. Environ. Int. 175, 107951. https://doi.org/10.1016/j.envint.2023.107951.

Zhou, T., Li, X., Liu, H., Dong, S., Zhang, Z., Wang, Z., Li, J., Nghiem, L.D., Khan, S.J., Wang, Q., 2024. Occurrence, fate, and remediation for per-and polyfluoroalkyl substances (PFAS) in sewage sludge: a comprehensive review. J. Hazard Mater. 466, 133637. https://doi.org/10.1016/j.jhazmat.2024.133637.